

# PCCP

Accepted Manuscript



This is an *Accepted Manuscript*, which has been through the Royal Society of Chemistry peer review process and has been accepted for publication.

*Accepted Manuscripts* are published online shortly after acceptance, before technical editing, formatting and proof reading. Using this free service, authors can make their results available to the community, in citable form, before we publish the edited article. We will replace this *Accepted Manuscript* with the edited and formatted *Advance Article* as soon as it is available.

You can find more information about *Accepted Manuscripts* in the [Information for Authors](#).

Please note that technical editing may introduce minor changes to the text and/or graphics, which may alter content. The journal's standard [Terms & Conditions](#) and the [Ethical guidelines](#) still apply. In no event shall the Royal Society of Chemistry be held responsible for any errors or omissions in this *Accepted Manuscript* or any consequences arising from the use of any information it contains.

## Plasma Induced Tungsten Doping to TiO<sub>2</sub> Particles for Enhancement of Photocatalysis under Visible Light

Cite this: DOI: 10.1039/x0xx00000x

Yohei Ishida,<sup>a</sup> Yasutomo Motokane,<sup>a</sup> Tomoharu Tokunaga,<sup>b</sup> and Tetsu Yonezawa<sup>a,\*</sup>

Received 00th January 2012,

Accepted 00th January 2012

DOI: 10.1039/x0xx00000x

www.rsc.org/

**Here we report a novel modification method of commercially available TiO<sub>2</sub> nanoparticles by a microwave-induced plasma technique. After the plasma treatment TiO<sub>2</sub> nanoparticles showed enhanced visible absorption due to the doped W atoms, and the photocatalytic methylene blue degradation above 440 nm was successfully improved.**

Titanium dioxide (TiO<sub>2</sub>) has been attracted much attention in wide research fields during the past decades due to its photocatalysis characterizaton.<sup>1,2</sup> TiO<sub>2</sub> is commercially available, cheap, and nontoxic photocatalysis that can decompose water or organic pollutants due to its excitation by the sunlight. One limitation of current TiO<sub>2</sub> photocatalysis is the non-responsiveness under visible light. TiO<sub>2</sub> is white powder and thus basically has absorption below 387 nm (corresponds to 3.2 eV of the band-gap for anatase crystals<sup>3</sup>). To utilize wide range of sunlight, visible-light responsive TiO<sub>2</sub> photocatalyst has been required. Recently the modification of TiO<sub>2</sub> toward the visible-light responsive photocatalyst is one of the main subjects in fields of photocatalyst<sup>1,4</sup>, green chemistry<sup>1,4</sup> and artificial photosynthesis.<sup>5</sup> Many modification strategies have been investigated including the introduction of oxygen vacancies<sup>6,7</sup>, and doping of hetero atoms such as Cr<sup>8</sup>, V<sup>8</sup>, N<sup>9</sup>, or S<sup>10</sup>.

The purpose of current work is to present a novel strategy to modify commercially available TiO<sub>2</sub> towards visible-light responsive photocatalyst. Recently a synthesis of metal nano-composites by plasma in liquid has been developed. The radio wavelength region (usually 13.56 MHz) has been used as the main source in the last decade<sup>11</sup>, but very recently microwave region (2.45 GHz) was newly used as more easily available source<sup>12-15</sup>. Plasma is easily produced with relatively small microwave equipment according to the high frequency of microwave. During the plasma production, bubbles continuously form and plasma is generated inside bubbles or around the bubble boundary in the liquid as reported in the previous paper.<sup>14,15</sup>

We have recently reported the synthesis of Ag,<sup>13</sup> Pt,<sup>13</sup> and ZnO<sup>12</sup> nanoparticles by using this microwave-induced plasma in aqueous solution containing metal ions. The mechanism for the metal nanoparticles formation is attributed to the reaction of metal ions with H<sup>•</sup> that comes from the decomposed water by plasma. According to these backgrounds, we herein report a novel

modification method of TiO<sub>2</sub> nanoparticles by using a microwave-induced plasma.

The modification of TiO<sub>2</sub> nanoparticles by microwave-induced plasma was carried out as described below. Among various TiO<sub>2</sub> nanoparticles, a commercially available decahedral TiO<sub>2</sub> nanoparticle (Showa Titanium Co. Ltd., decahedral TiO<sub>2</sub><sup>16</sup>) was used because an easy observation of its crystal phase is expected by a high magnification scanning transmission electron microscopy (STEM).

A home made microwave-induced liquid plasma system (see Figure S1) was used for the synthesis. 2 g of decahedral TiO<sub>2</sub> powder was dispersed in 500 mL of deionized water (> 18.2 MΩ prepared by an Organo/ELGA purelabo system). Into this aqueous suspension, microwave plasma was introduced at 400 W for various periods from 5 to 40 min under a reduced pressure (< 2.1 10<sup>4</sup> Pa) using a diaphragm pump. After the plasma reaction, the resultant suspension was filtered by membrane filter (ADVANTEC, 1.0 μm of pore size) and dried for over night. Yellowish powder (see Figure S2) was obtained after 40 min plasma reaction.

First, the obtained TiO<sub>2</sub> powder was characterized by XRD as shown in Figure 1. Most importantly, characteristic peaks of TiO<sub>2</sub> were observed at 24-30 and 52-58 degrees. Bare decahedral TiO<sub>2</sub> showed sharp patterns of anatase crystal at 25.2, 37.3, 48.0, 53.7, 55.0, 62.5, 67.3, 70.0, 74.5, and 81.7 degrees, as well as relatively weak rutile peaks at 26.4 and 35.2 degrees. Since these peaks were also observed after plasma treatment for 5 to 40 min and did not change, it is estimated that the crystal structure was maintained even during the plasma treatment. After 40 min of plasma treatment (red line in Figure 1), small patterns corresponding tungsten components were detected at 23.2, 26.2, around 35, and 40.2 degrees (WO<sub>3</sub>) and at 10.5, 42.5, and 45.2 degrees (H<sub>2</sub>WO<sub>4</sub>·H<sub>2</sub>O), respectively. These W components were contaminated from the electrode used in the plasma equipment (see Figure S1). In fact, the surface of W electrode was slightly damaged after plasma irradiation. To obtain pure Ti components and investigate the accurate characteristics, we examined to remove the W components by alkaline solution. Tungsten oxides can be readily dissolved into aqueous alkaline. It is known that nano W components are easily oxidized and resultant oxides can dissolve in concentrated NaOH aqueous solution.<sup>17</sup> We introduced 300 mL of NaOH solution (ca. pH 13) into 1.0 g of resultant TiO<sub>2</sub> powder and stirred for 30 min. It was filtered and repeatedly washed with deionized water. The XRD patterns of W

components disappeared completely after the alkaline treatment (yellow line), thus we succeeded in the purification of plasma-modified TiO<sub>2</sub> powders. Yellowish color of as-prepared TiO<sub>2</sub> nanoparticles (plasma for 40 min) turned to light ashy (see Figure S2) by the alkaline treatment. This color change is attributed to the removal of yellowish WO<sub>3</sub> and H<sub>2</sub>WO<sub>4</sub>·H<sub>2</sub>O, those usually have absorption below 500<sup>18</sup> and 520<sup>18</sup> nm, respectively. All samples were successfully purified by the same procedure. Their XRD patterns are summarized in Figure 1.

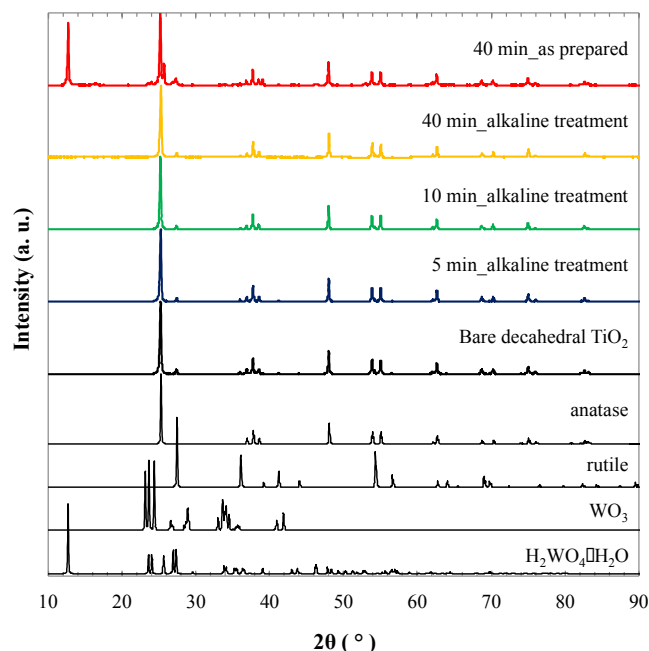


Figure 1. XRD patterns of plasma-modified decahedral TiO<sub>2</sub> nanoparticles. References were obtained from JCPDS data: anatase (00-021-1272), rutile (00-021-1276), WO<sub>3</sub> (00-032-1395), and H<sub>2</sub>WO<sub>4</sub>·H<sub>2</sub>O (00-018-1420).

Figure 2a-c shows high-angle annular dark-field scanning transmission electron microscopic (HAADF-STEM) image of bare decahedral TiO<sub>2</sub> (a), after plasma reaction for 40 min without (b) and with (c) the alkaline treatment. Around 50 to 250 nm of particle diameter with decahedral structures were observed in these 3 images as reported in the previous paper.<sup>16</sup> From these HAADF-STEM images, we can conclude that the particle size and shape of our TiO<sub>2</sub> did not change during the plasma and alkaline treatments.

High magnification HAADF-STEM images are shown in Figure 2d-f. HAADF-STEM method enables to observe the chemical contrast according to the atomic number (*Z*). In the present case, the atomic number of <sup>22</sup>Ti is much smaller than that of <sup>74</sup>W, thus the contaminated W components can be detected. The bare decahedral TiO<sub>2</sub> nanoparticle has a flat surface with an atomic precision (Figure 2d). After the plasma treatment, the surface became rough (sometimes called “damaged surface”) and the contrast of the surface is much higher than that of inner region (Figure 2e). The rough surface should be derived from the extremely high temperature of plasma (several thousands °C). Since the melting point of TiO<sub>2</sub> is *ca.* 1840 °C,<sup>19</sup> current experimental temperature may melt the surface of TiO<sub>2</sub> particles. After the alkaline treatment, we did not observe any high-contrast surfaces (Figure 2f), and rough surfaces remained. The removal of high-contrast layer is attributed to the purification of W components on the particle surface by the alkaline treatment. However, even after the alkaline treatment we

still observed a bright spots on the particle region as indicated by red arrows in Figure 2f. These spots should be composed of heavier atoms than the backgrounds (Ti and O), thus they are estimated to be the doped W atoms introduced from the electrode of the plasma equipment.

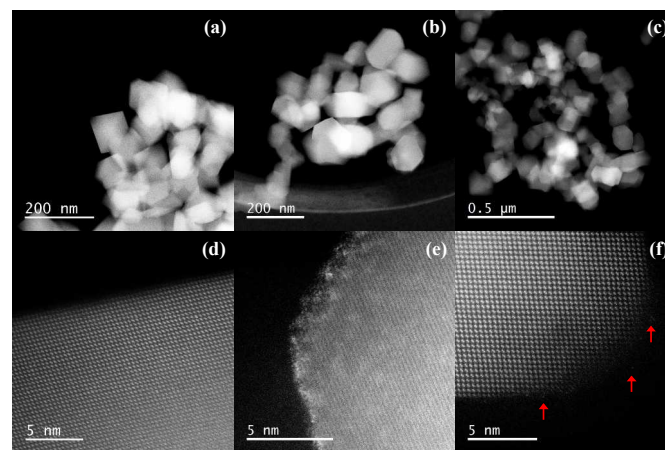


Figure 2. HAADF-STEM images of decahedral bare TiO<sub>2</sub> powder (a, d), after the 40 min alkaline treatment without (b, e) and with (c, f) alkaline treatment.

In order to determine the loading amount of W atoms in TiO<sub>2</sub> nanoparticles, inductively coupled plasma atomic emission spectroscopy (ICP-AES) was carried out (see the experimental procedure in SI). As a result, the atomic percent of W (= W/Ti × 100%) was determined to be 0.0, 0.1, 0.2, and 0.2% for 0 (bare), 5, 10, and 40 min samples, respectively. The loading amount seemed to be saturated at 10 min of plasma treatment. This phenomenon will be discussed with diffuse reflectance spectra (Figure 3). STEM energy-dispersive X-ray spectroscopy (EDX) analysis was also carried out (Figure S3). The plasma-treated decahedral TiO<sub>2</sub> particles obviously showed the W component on their surfaces (before the alkaline treatment, Figure S3a). On the other hand, the surface W components were eliminated after the alkaline treatment (Figure S3b). These observations strongly support the discussions by XRD (Figure 1) and STEM (Figure 2) results. It should be noted that we still observed weak, but enough strong W components even after the alkaline treatment. The counts of W mapping were rather stronger than the backgrounds. Therefore we concluded that W atoms were doped inside the TiO<sub>2</sub> crystal structure from the electrode of the plasma equipment, as we discussed with Figure 2f and ICP-AES. The ionic radii of Ti and W are 60.5 and 60 pm,<sup>20</sup> respectively, thus the W atom should be able to substitute for Ti atom in the crystal structure. These ICP-AES and STEM-EDX results clearly indicate that microwave-induced plasma technique can dope W atoms into TiO<sub>2</sub> nanoparticles.

The photocatalysis performance of our plasma-modified decahedral TiO<sub>2</sub> nanoparticles was investigated below. First the diffuse reflectance spectra were recorded for 300–800 nm with a baseline of BaSO<sub>4</sub> as shown in Figure 3 (also see the spectra for 300–2000 nm in Figure S4). The bare decahedral TiO<sub>2</sub> does not have visible light reflectance over 400 nm (black line). On the other hand, visible light reflectance arose after the plasma treatment. This reflectance enhancement is probably derived from the doping of W atoms as observed in Figure 2. It is known that conduction band of TiO<sub>2</sub> gradually moves downward with the increase of W loading amount below 2%, that basically result in the red shift of absorption.<sup>21</sup> The as-prepared plasma TiO<sub>2</sub> (40 min, red line) showed a characteristic absorption around 400–500 nm, and it disappeared

after the alkaline treatment (yellow line). It is known that  $\text{WO}_3$  and  $\text{H}_2\text{WO}_4 \cdot \text{H}_2\text{O}$  have their characteristic absorption at 500 and 520 nm,<sup>18</sup> respectively. Thus, diffuse reflectance spectra also support the successful purification of W components. Visible light reflectance of 10 and 40 min samples were almost similar. This result suggests that the effect of plasma on the absorption enhancement of decahedral  $\text{TiO}_2$  nanoparticles was saturated. This result agrees with the same loading amount of W determined by ICP–AES. Judging from their reflectance, *ca.* 12% enhancement of reflectance at 600 nm from bare  $\text{TiO}_2$  is the saturation point by the current plasma treatment (5 min was not saturated as can be understood from the blue line). The plausible reason for the saturation is the large particle diameter of current decahedral  $\text{TiO}_2$  nanoparticles (50–250 nm<sup>16</sup>). Such large particles have relatively small specific surface areas and the total rate for modification in the surface regions should be limited. Our preliminary experiment of similar liquid plasma for smaller  $\text{TiO}_2$  nanoparticles (ISK, ST-01, *ca.* 5 nm of particle diameter determined by TEM) showed much drastic enhancement in their visible-light reflectance (not shown). These results will be reported soon. Synthesis of visible-light responsive  $\text{TiO}_2$  nanoparticles is now attracted much attention as a future photocatalysis utilizes wide wavelength regions of sunlight. Our liquid plasma method thus will widen the spectrum of the modification strategy towards functionalized  $\text{TiO}_2$  nanoparticles.

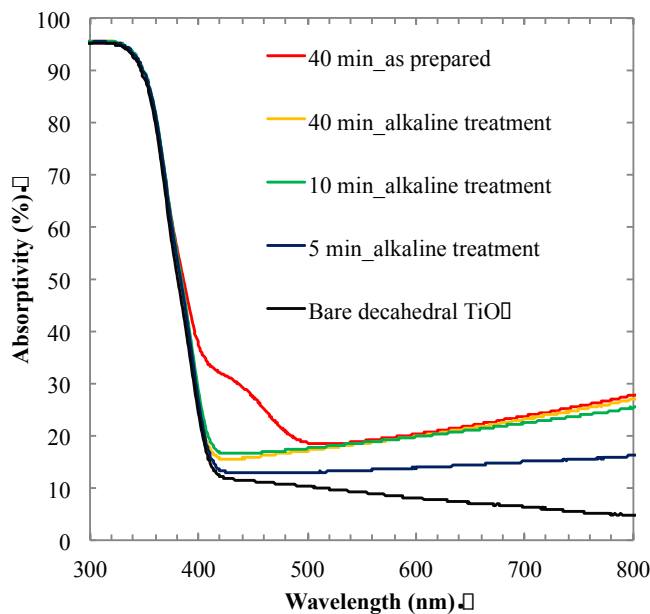


Figure 3. UV-Vis diffuse reflectance spectra of decahedral  $\text{TiO}_2$  nanoparticles.

The photocatalysis performance of our decahedral  $\text{TiO}_2$  nanoparticles was preliminary investigated by the methylene blue (MB) degradation test under visible-light irradiation.<sup>2</sup> Hg-Xe lamp (San-ei electric, UVF-204S, 200 W) was used as an excitation light source with an optical cut filter for  $< 440$  nm. The experimental procedure is below. 50 mg of  $\text{TiO}_2$  powder was dispersed in the 40 mL of 10 mg L<sup>-1</sup> MB aqueous solution. The mixture was stirred for 30 min under dark. 1 mL of the sample was taken and centrifuged at 6300 rpm for 3 min to precipitate the  $\text{TiO}_2$  powders. Supernatant was put in a quartz cell with a 1 mm of optical path, and we measured the absorption spectrum (Shimadzu, UV-1800) in order to determine the initial concentration of MB. Irradiation was then started, and we measured the absorption spectra of supernatant in each 30 min.

The degradation of MB could be analyzed by first-order kinetics, with the classical equation of  $\ln(C_0/C) = kt$ , where  $C_0$  and  $C$  indicate the absorbance at 665 nm before and after the irradiation, respectively,  $k$  is the rate constant and  $t$  is the irradiation time. Figure 4 shows the concentration change of MB  $\ln(C_0/C)$  as a function of irradiation time. Figure S5 in SI shows the raw absorption spectral change during the excitation. As can be seen from Figure 4, it is obvious that the plasma-treated  $\text{TiO}_2$  showed better performances than that of bare decahedral  $\text{TiO}_2$ . The reaction rate constants ( $k$ ) of bare, 10 and 40 min plasma-treated  $\text{TiO}_2$  were  $2.3 \times 10^3$ ,  $2.6 \times 10^3$  and  $2.8 \times 10^3$  min<sup>-1</sup>, respectively. From these values, it is expected that the longer plasma time result in better photocatalytic performance under visible light. These photocatalytic enhancements were not derived from the specific surface areas (the particle size and shape remained as shown in Figure 2), and the enhanced visible-light reflectance should be the main reason. We conclude that the liquid plasma technique enables to produce visible-light responsive photocatalysis by easy and simple way. Although the loading amount of W into  $\text{TiO}_2$  nanoparticles and photocatalytic performance were almost saturated at 10 min (from ICP and UV-Vis results), larger specific surface area of  $\text{TiO}_2$  nanoparticles or stronger plasma power may result in larger amount of W doping the nanoparticles.

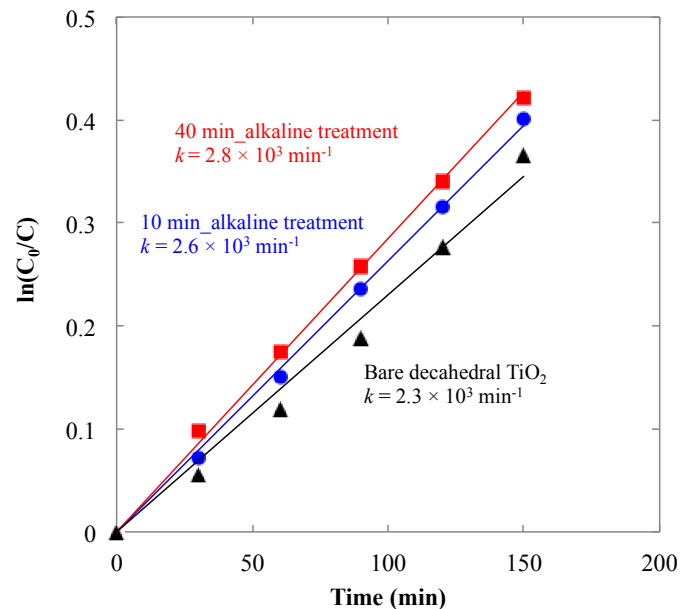


Figure 4. MB degradation under the irradiation above 440 nm.  $C_0$  and  $C$  indicate the absorbance at 665 nm after and before the irradiation, respectively.  $k$  indicates the photocatalysis reaction rate constant.

In conclusion, we presented a novel modification procedure of commercially available decahedral  $\text{TiO}_2$  nanoparticles by a microwave-induced plasma. The size and shape of decahedral  $\text{TiO}_2$  did not change during the plasma treatment. The damaged surface layer was observed after the plasma treatment, moreover the doping of W atoms in the  $\text{TiO}_2$  structure was expected from the high magnification HAADF-STEM and EDX mapping. Attributed to the enhancement of visible-light reflectance, the photo-catalytic methylene blue degradation above 440 nm of irradiation was successfully improved. Simple and easy procedure presented here therefore will widen the modification strategy towards functionalized  $\text{TiO}_2$  photocatalyst.

### Experimental Section

The microwave generator is a UW-1500 (Micro-Denshi, Japan) at 2.45 GHz. Microwaves were emitted from the magnetron pass through a WRJ-2 rectangular wave guide ( $109.22 \times 54.61$  mm), a power meter, a tuner, and a waveguide to the coaxial adaptor. The electrodes were made of tungsten (Experimental setup was illustrated in Figure S1). For characterization, XRD (Rigaku, MiniFlexII), STEM-HAADF (JEOL, JEM-ARM200, acceleration voltage of 200 kV), STEM-EDX (FEI, TITAN III G2 Cubed, 300 kV), diffuse reflectance spectroscopy (JASCO, V-670) were used. ICP-AES was measured with Thermo SCIENTIFIC iCAP 6000.

### Acknowledgement

This work was partly supported by a Research Fund from Hokkaido University to YI and TY, and by Grant-in-Aid for Scientific Research (A) from JSPS (24241041). This work was also partially supported by Hokkaido University, microstructural characterization platform as a program of Nanotechnology Platform of the Ministry of Education, Culture, Sports, Science and Technology (MEXT), Japan. Authors thank Prof. B. Ohtani (Hokkaido Univ.) for the fruitful discussion. A part of this work was also supported by the Advanced Characterization Nanotechnology Platform of the National Institute for Materials Science and the High Voltage Electron Microscopy Laboratory of Nagoya University.

### Notes and references

<sup>a</sup> Division of Material Science and Engineering, Faculty of Engineering, Hokkaido University, Kita 13 Nishi 8, Kita-ku, Sapporo, Hokkaido 060-8628, Japan.

<sup>b</sup> Department of Quantum Engineering, Graduate School of Engineering, Nagoya University, Furo-cho, Chikusa-ku, Aichi, Nagoya 464-8603, Japan

\*Corresponding author E-mail address: tetsu@eng.hokudai.ac.jp

Electronic Supplementary Information (ESI) available: detailed experimental procedures. See DOI: 10.1039/c000000x/

- 1 A. Fujishima, K. Honda, *Nature*, 1972, **238**, 37.
- 2 C. Xue, T. Narushima, Y. Ishida, T. Tokunaga, T. Yonezawa, *ACS Appl. Mater. Interfaces*, 2014, **6**, 19924.
- 3 H. Tang, K. Prasad, R. Sanjines, P. E. Schmid, F. Levy, *J. Appl. Phys.*, 1994, **75**, 2042.
- 4 A. Fujishima, T.N. Rao, D.A. Tryk, *J. Photochem. Photobiol. C*, 2000, **1**, 1.
- 5 S. Okunaka, H. Tokudome, Y. Hitomi, R. Abe, *J. Mater. Chem. A*, 2015, **3**, 1688.
- 6 X. Chen, L. Liu, P. Y. Yu, S. S. Mao, *Science*, 2011, **331**, 746.
- 7 I. Nakamura, N. Negishi, S. Kutsuna, T. Ihara, S. Sugihara, K. Takeuchi, *J. Mol. Catal. A*, 2000, **161**, 205.
- 8 M. Anpo, M. Takeuchi, *Inter. J. Photoenergy*, 2001, **3**, 89.
- 9 R. Asahi, T. Morikawa, T. Ohwaki, K. Aoki, Y. Taga, *Science*, 2001, **293**, 269.
- 10 T. Umebayashi, T. Yamaki, H. Itoh, K. Asai, *Appl. Phys. Lett.*, 2002, **81**, 154.
- 11 T. Ihara, M. Miyoshi, M. Ando, S. Sugihara, Y. Iriyama, *J. Mat. Sci.*, 2001, **36**, 4201.
- 12 T. Yonezawa, A. Hyono, S. Sato, O. Ariyada, *Chem. Lett.*, 2010, **39**, 783.

- 13 S. Sato, K. Mori, O. Ariyada, A. Hyono, T. Yonezawa, *Surf. Coat. Tech.*, 2011, **206**, 955.
- 14 S. Nomura, H. Toyota, M. Tawara, H. Yamashita, K. Matsumoto, *Appl. Phys. Lett.*, 2006, **88**, 231502.
- 15 S. Nomura, *J. Plasma Fusion Res.*, 2013, **89**, 199.
- 16 F. Amano, O. O. P. Mahaney, Y. Terada, T. Yasumoto, T. Shibayama, B. Ohtani, *Chem. Mater.*, 2009, **21**, 2601.
- 17 R. Jedamzik, A. Neubrand, J. Rödel, *J. Mater. Sci.*, 2000, **35**, 477.
- 18 J. Cao, B. Luo, H. Lin, B. Xu, S. Chen, *Appl. Catal. B*, 2012, **111**, 288.
- 19 J. Hlavac, *Pure Appl. Chem.*, 1982, **54**, 681.
- 20 R. D. Shannon, *Acta. Cryst.*, 1976, **A32**, 751.
- 21 Z. Xi, L. Fang, H. L. Qiu, Z. Gang, W. S. Zhong, *J. Phys. Chem. C* 2011, **115**, 12665.